Penerbit Akademia Baru

Journal of Advanced Research in Fluid Mechanics and Thermal Sciences

Journal homepage: www.akademiabaru.com/arfmts.html
ISSN: 2289-7879

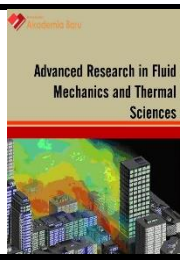

Effect of MHD and Porous Media on Nanofluid Flow with Heat Transfer: Numerical Treatment

Open Access

Rabiha Saleem Kareem[1,*], Ahmed M. Abdulhadi[1]

[1] Department of Mathematics, College of Science, Baghdad University, Baghdad, Iraq

ARTICLE INFO

Article history:
Received 23 August 2019
Received in revised form 26 September 2019
Accepted 4 October 2019
Available online 30 November 2019

Keywords:
Peristalsis flow; nanofluid; asymmetric tube; porous medium; magnetic field

ABSTRACT

The present article studies nanofluids flow and heat transfer in a vertical asymmetric tube in the presence of a magnetic field and porous media under peristaltic waves so flow equations are modeled considering cylinder coordinates. With low Reynolds number (effects inertial force is negligible) and lengthy wavelength, the governing equations (mass, motion, energy) are derived with appropriate boundary conditions on the walls. The exact solution is obtained for energy equation whereas velocity equation is solved numerically by Runge- Kutta method. The influence of numerous parameters such as Grashof number, Hartmann number, heat source parameter, viscosity parameter, Darcy number, nanoparticle volume fraction, the phase difference and amplitudes of left and right walls are discussed in respect of velocity, temperature and heat transfer coefficient. The results are obtained by Mathematica 11 program.

1. Introduction

Peristaltic transport is a phenomenon that happens when expansion and contraction of a flexible tube in a fluid generate consecutive waves which transmit along the length of the tube. This phenomenon has become a topic of great for biomedical, industrial application and physiological.

It has a wide application in physiological fluid transport in biological regulation such as the work the kidney to a bladder, movement food in digestive system, movement of ovum in fallopian channel, transference of lymph during the lymphatic vessels and blood flow in tiny vessels.

* *Corresponding author.*
E-mail address: Rabiha_s77@yahoo.com (Rabiha Saleem Kareem)

Moreover, there are numerous engineering practicability as well in which peristaltic Machines are used to transport a vast range of fluids principally in the pharmaceutical industries and chemical. The active studies in peristaltic flow by Shapiro *et al.,* [1] and Latham [2]. Analysis on the peristaltic flow through eccentric cylinders have been discussed theoretically and experimentally by Mekhemer *et al.,* [3] moreover Nadeem *et al.,* [4]. Reddy *et al.,* [5] has stated the work on the peristaltic flow of a viscous conducting fluid a vertical asymmetric channel. Hayat *et al.,* [6] studied the peristaltic flow for the Newtonian fluid in an endoscope and debated the exact solution.

Peristaltic flow through magnetic fields has been taken a great interest before the students and researchers consequent to its expanded implementation in astrophysics and geophysics etc. It was noticed that a magnetic field was able of controlling the thickening of viscosity of fluid. Moreover, the magnetic field was very important in identifying and therapy of hypothermia, tumors and intestinal sicknesses. Several scientific researchers studied peristaltic motion under influence magnetic field [7-10].

Nanofluids are manufacture by suspending nanoparticles which may be metallic/non-metallic in base fluids and have been used in a wide range of technologies several of which have been studied by many of researcher. In modern years, great effort has been given to the study of nanofluids. In modern years, great labor has been given to the nanofluids research. Investigate researches [11–14] appeared that even for a tiny volumetric portion of nanoparticles, the thermic conductivity of the base fluid is improved by (10–50) % with a notable the convective heat transfer coefficient is increase. Das *et al.,* [15] have seen that the thermic conductivity for nanofluids rises with growing temperature. Heris *et al.,* [16] experimentally studied the convective heat transfer coefficient of CuO-water and Al_2O_3-water nanofluids for laminar flow with tube in a constant wall temperature boundary condition. Naheeda *et al.,* [17] discussed the effect of wall properties and Cu-water nanofluid in a non-uniform inclined tube. Effect of heat transfer with the non-Newtonian fluid containing gold nanoparticles in tube discussed by Mekheimer *et al.,* [18]. Synchronous impacts of wall and slip properties have been studied by Aly and Ebaid [19] and Hayat *et al.,* [20] analyzed an impact on entropy generation peristaltic flux of nanoparticles in a rotational frame.

Peristaltic flow through porous medium is very common in numerous biological processes such as transportation the urine through ureter with stones. In some pathological cases, the porous medium can be seen while the arteries are closed due to oil cholesterol or blood masses. Hussein *et al.,* [21] investigated the peristaltic flow of MHD through porous medium during asymmetric channels. Mekheimer [22] studied peristaltic flow through a porous medium in a tended planar tube. Salman and others [23] Analyzed the heat and mass transfer in in inclined asymmetric channel through porous medium under Influence magnetic field.

In this study, the aim has been to analysis heat, heat transfer coefficient and fluid flow of peristaltic in a vertical asymmetric tube with existing a porous medium, magnetic field, a variable viscosity reliant on a fluid temperature and nanoparticles. Water is base fluid and Copper oxide-water nanoparticles are merged. The governing equations are simplified under the lengthy wavelength and low Reynolds number. Finally, graphical study has been done to figure out the effect of some important parameters containing in the above functions in details.

2. Formulation of the Problem

Investigate the peristaltic flow of nanofluids in asymmetric vertical circular tube of width $(d_1 + d_2)$ and length L with variable viscosity. The tube filled with porous medium, $k1$. The tube walls are elastic and the flow is observed by the peristaltic sinusoidal waves move with velocity c, propagating on lengthwise the walls of the channel. The cylindrical coordinates (R, Z) are considered in such Z-axis is taken as the center line of the tube while R-axis is vertical to it. The geometry of the walls surface is stated as follows

$$\bar{h}_1 = a_1 + b_1 \cos\left(\frac{2\pi}{\lambda}(\bar{Z} - c\bar{t})\right) \tag{1}$$

$$\bar{h}_2 = a_2 + b_2 \cos\left(\frac{2\pi}{\lambda}(\bar{Z} - c\bar{t}) + \varphi\right) \tag{2}$$

where h_1 and h_2 are the left and right tube wall respectively, $b_1$and b_2 are the amplitudes of the walls ,λ is the wavelength, the phase difference φ , $\bar{t}$ is the time and $\bar{Z}$ is the direction of the wave propagation. Let $\bar{u}(\bar{r}, \bar{z})$ and $\bar{w}(\bar{r}, \bar{z})$ are represent the components of velocity in the axial r and z directions respectively. The flow filed in laboratory frame is unsteady becomes steady in wave frame. The relation between the two frames are given by

$$\bar{r} = \bar{R},\ \bar{z} = \bar{Z} - c\bar{t}\ , \bar{v} = \bar{V},\ \ \bar{w} = \bar{W}, \bar{p}(\bar{z}, \bar{r}, \bar{t}) = \bar{P}(\bar{Z}, \bar{R}, \bar{T}) \tag{3}$$

Now, the basic equations governing the motion and heat for the vertical tube are

$$\frac{1}{r}\frac{\partial \bar{u}}{\partial \bar{r}} + \frac{\partial \bar{w}}{\partial \bar{z}} = 0 \tag{4}$$

$$\rho_{nf}\left[\bar{u}\frac{\partial \bar{u}}{\partial \bar{r}} + \bar{w}\frac{\partial \bar{u}}{\partial \bar{z}}\right] = -\frac{\partial \bar{p}}{\partial \bar{r}} + \frac{\partial}{\partial \bar{r}}\left[2\mu_{nf}(\theta)\frac{\partial \bar{u}}{\partial \bar{r}}\right] + \mu_{nf}(\theta)\frac{2}{r}\left(\frac{\partial \bar{u}}{\partial \bar{r}} - \frac{\bar{u}}{\bar{r}}\right) +$$

$$\frac{\partial}{\partial \bar{z}}\left[\mu_{nf}(\theta)\left(\frac{\partial \bar{u}}{\partial \bar{r}} + \frac{\partial \bar{w}}{\partial \bar{z}}\right)\right] - \mu_{nf}(\theta)\frac{\bar{u}}{k}, \tag{5}$$

$$\rho_{nf}\left[\bar{u}\frac{\partial \bar{w}}{\partial \bar{r}} + \bar{w}\frac{\partial \bar{w}}{\partial \bar{z}}\right] = -\frac{\partial \bar{p}}{\partial \bar{z}} + \frac{1}{r}\frac{\partial}{\partial \bar{r}}\left[\mu_{nf}(\theta)\bar{r}\left(\frac{\partial \bar{u}}{\partial \bar{z}} + \frac{\partial \bar{w}}{\partial \bar{r}}\right)\right] + \frac{\partial}{\partial \bar{z}}\left[2\mu_{nf}(\theta)\left(\frac{\partial \bar{w}}{\partial \bar{z}}\right)\right] +$$

$$(\rho\gamma)_{nf} g(\bar{T} - T_0) - \sigma\beta_0^2\bar{w} - \mu_{nf}(\theta)\frac{\bar{w}}{k}, \tag{6}$$

$$\frac{\partial \bar{T}}{\partial \bar{t}} + \bar{u}\frac{\partial \bar{T}}{\partial \bar{r}} + \bar{w}\frac{\partial \bar{T}}{\partial \bar{z}} = \frac{k_{nf}}{(\rho_{cp})_{nf}}\left[\frac{\partial^2 \bar{T}}{\partial \bar{r}^2} + \frac{1}{\bar{r}}\frac{\partial \bar{T}}{\partial \bar{r}} + \frac{\partial^2 \bar{T}}{\partial \bar{z}^2}\right] + \frac{Q_0}{(\rho_{cp})_{nf}}. \tag{7}$$

where $\bar{r}$ and $\bar{z}$ are the coordinates in the wave frame.$\bar{T}$ is the temperature of the fluid. β_0 the magnitude of magnetic field. The Maxwell-Garnet model for effective thermal conductivity (k_{nf}) used in the current flow problem is described as [24]

$$k_{nf} = k_f \left(\frac{k_n + 2k_f - 2\phi(k_f - k_n)}{(k_n + 2k_f + 2\phi(k_f - k_n)} \right) \tag{8}$$

The effective thermal diffusivity of nanofluid (α_{nf}) , the effective density of nanofluid (ρ_{nf}) , capacitance respectively of consider nanofluid $(\rho c_p)_{nf}$ and the thermal expansion coefficient (γ_{nf}) of considered nanofluid for flow model is defined as [24]

$$\begin{aligned} &\alpha_{nf} = \frac{k_{nf}}{(\rho c_p)_{nf}} \, , \rho_{nf} = (1-\phi)\rho_f + \phi\rho_n \, , \\ &(\rho c_p)_{nf} = (1-\phi)(\rho c_p)_f + \phi(\rho c_p)_n \, , \\ &(\rho\gamma)_{nf} = (1-\phi)(\rho\gamma)_f + \phi(\rho\gamma)_n . \end{aligned} \tag{9}$$

In above equations ρ , c_p and k define the density, thermal expansion coefficient, specific heat and thermal conductivity. The subscripts f and n denoted the base fluid (water) and nanofluid (CuO), respectively.

The effective dynamic viscosity (μ_{nf}) due Reynolds model is mathematically written as

$$\mu_{nf} = \frac{\mu_f e^{-\alpha\theta}}{(1-\phi)^{2.5}} \text{ and } e^{-\alpha\theta} = 1 - \alpha\theta \ , \ \alpha << 1 \ . \tag{10}$$

where (μ_f) is viscosity of the fluid, (α) is the viscosity parameter and (ϕ) is the nanoparticle volume fraction. The following non-dimensional variables

$$r = \frac{\bar{r}}{a_1} , \ z = \frac{\bar{z}}{\lambda} , \ w = \frac{\bar{w}}{c} , \ u = \frac{\lambda \bar{u}}{a_1 c} , \ p = \frac{{a_1}^2 \bar{p}}{c\lambda\mu_f} , \ \theta = \frac{(\bar{T} - \bar{T}_0)}{\bar{T}_0} \ , h_1 = \frac{\bar{h}_1}{a_1} ,$$

$$h_2 = \frac{\bar{h}_2}{a_1} , t = \frac{c\bar{t}}{\lambda} , \ \varepsilon_1 = \frac{b_1}{a_1} , \ \varepsilon_2 = \frac{b_2}{a_1} , \ a = \frac{a_2}{a_1} , \ Re = \frac{\rho a_1 c}{\mu_f} , \ Gr = \frac{g\alpha {a_1}^2 T_0 \rho_f}{c\mu_f} ,$$

$$\beta = \frac{{a_1}^2 Q_0}{T_0 k_f} , \ M^2 = \frac{\beta_0^2 a_1^2 \sigma}{\mu_f} , K = \frac{k_1}{{a_1}^2} , \ \delta = \frac{a1}{\lambda} . \tag{11}$$

Here r and z are dimensionless $\bar{r}$, $\bar{z}$ coordinates, t is dimensionless time, w and u are dimensionless axial and transverse velocity components, p is dimensionless pressure, θ is dimensionless temperature function, ε_1 and ε_2 are amplitudes of left and right walls, δ is the wave number , Re is the Reynolds number , Gr Grashof number , β is heat source/sink parameter, M is the Hartmann number and K is the Darcy number. By substituting Eq. (11) in Eq. (5) to (7) and under the suppositions of long wave length $\delta \ll 1$ and low Reynolds number. We obtain

$$\frac{\partial p}{\partial r} = 0 \ , \tag{12}$$

$$\frac{\partial p}{\partial z} = \frac{1}{r} \frac{\partial}{\partial r} \left(\frac{\mu_{nf}}{\mu_f} \left(r \frac{\partial w}{\partial r} \right) \right) + \frac{(\rho\gamma)_{nf}}{(\rho\gamma)_f} Gr\theta - \left(M^2 + \frac{\mu_{nf}}{\mu_f K} \right) w, \tag{13}$$

$$\frac{\partial^2\theta}{\partial r^2}+\frac{1}{r}\frac{\partial\theta}{\partial r}+\beta\frac{k_f}{k_{nf}}=0\,. \tag{14}$$

The dimensionless of boundary conditions are defined as

$$w=-1 \quad ,\theta=0 \qquad \text{at } r=h_1(z) \text{ where } h_1=1+\varepsilon_1\cos(2\pi z) \tag{15}$$

$$\frac{\partial w}{\partial r}=0 \quad , \frac{\partial\theta}{\partial r}=0 \qquad \text{at } r=h_2(z) \text{ where } h_2=a+\varepsilon_2\cos(2\pi z+\varphi) \tag{16}$$

Heat transfer coefficient at the left and right walls are defined as equations

$$z_{h1}(r)=\frac{k_{nf}}{k_f}\left(\frac{\partial\theta}{\partial r}\right)_{r=h1} \qquad \text{left wall} \tag{17}$$

$$z_{h2}(r)=\frac{k_{nf}}{k_f}\left(\frac{\partial\theta}{\partial r}\right)_{r=h2} \qquad \text{right wall} \tag{18}$$

3. Solution of The Problem

Solving Eq. (14) with boundary conditions in (15) and (16), we obtain the expression for temperature as follows

$$\theta(r,z)=-\frac{1}{4}\left(\frac{k_n+2k_f+2\phi(k_f-k_n)}{(k_n+2k_f-2\phi(k_f-k_n)}\right)r^2\beta+\mathrm{c}_2+c_1\log(r)\,, \tag{19}$$

where

$$\mathrm{c}_1=\frac{1}{2}\left(\frac{k_n+2k_f+2\phi(k_f-k_n)}{(k_n+2k_f-2\phi(k_f-k_n)}\right)h_2^2\beta \tag{20}$$

$$c_2=\frac{1}{4}\left(\left(\frac{k_n+2k_f+2\phi(k_f-k_n)}{(k_n+2k_f-2\phi(k_f-k_n)}\right)h_1^2\beta-2\left(\frac{k_n+2k_f+2\phi(k_f-k_n)}{(k_n+2k_f-2\phi(k_f-k_n)}\right)h_2^2\beta\,log(h_1)\right) \tag{21}$$

Eq. (13) with boundary conditions (15) and (16) is solved numerically in Mathematica. This technique is based on the Runge-Kutta method with 4th order. Graphical analysis is presented in the next section.

4. Result and Conclusion

Objective of this part is to investigate the impact of diverse physical parameters on the velocity distribution, temperature distribution and heat transfer coefficient with illustrate by graphical results presented in Figure 1-19. The parameters contain the Grashof number, the Hartmann number, the Darcy number, heat source parameter, viscosity parameter, nanoparticle volume

fraction, the phase difference and the amplitudes of left and right walls. These calculations are founded on nanofluid properties authenticated in Table 1.

Table 1
Thermo - physical properties of H_2O & CuO

Physical properties	$c_p(J/kgK)$	$\rho(kg/m^3)$	$k\ (W/mk)$	$\gamma * 10^{-5}(1/K)$
H_2O	4179.0	997.1	0.613	21.0
CuO	540.0	6500.0	18.0	0.85

4.1 Velocity Profile

Figure 1-9 describes the velocity profile w, as a function of (r), for numerous values of parameters, where the other parameters are static. Figure 1 shows the effect of viscosity parameter (α) on the velocity profile, the velocity is increasing near to walls with increases of (α) values, but the velocity is nearly not affected by enhancement of this parameter in center of the tube .The influence of the Darcy number (K) and the heat source/sink parameter (β) were shown in Figure 2 and 3. Notice that higher values of the Darcy number and the heat source/sink parameter decrease the velocity in the center of the tube but the situation is inverted by the side of the tube walls. In addition, Figure 4 reveal that as Grashof number (Gr) increase, the velocity profile increases close to the walls of tube whereas it not effects at the central of the tube. In Figure 5, one can note that the axial velocity rises with an increase in amplitudes of left wall (ε_1). Figure 6 displays that the increase in nanoparticle volume fraction (ϕ) decreases the fluid velocity at the right wall of the channel while Gradually effect of this parameter decreasing towards middle and left wall. Figure 7 and Figure 8 are depicted to study the influence of amplitudes of right wall (ε_2) and the phase difference (φ). these figures mention that an increase in (ε_2) and (φ) the axial velocity decreases near the left wall for ($0 < r < 0.976$) . While the velocity increases in the rest of the tube with values of ($0.976 < r$). Also, Figure 9 designates that the great values of the Hartmann number (M) reduce the velocity at the walls of the tube and the influence of this parameter is progressively fading in the core of the tube. this result is expecting because the realty that an impact of magnetic field produces a Lorentz force that is a resistant force.

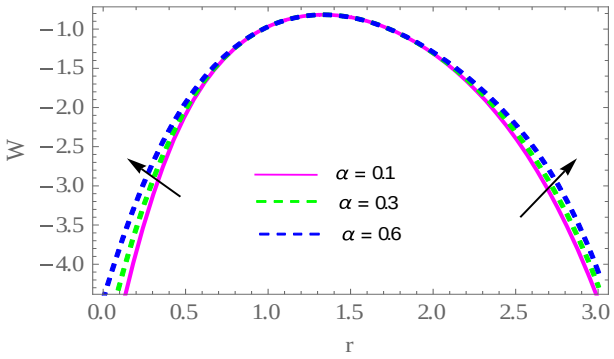

Fig. 1. Velocity distribution with different values of (α) z=0.7, Gr= 2.0, ϕ = 0.04, β = 2, $\frac{\partial p}{\partial z}$ = 0.2, φ = π/3, $\varepsilon_1 = 0.1$, $\varepsilon_2 = 0.5$, K= 0.5, M=1

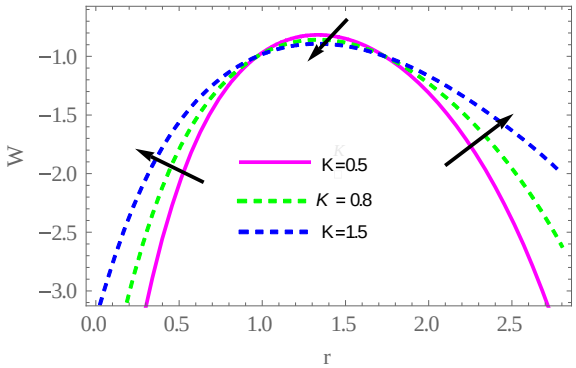

Fig. 2. Velocity distribution with different values of (K) z= 0.7, Gr= 2.0, $\phi = 0.04$, $\beta = 2$, $\frac{\partial p}{\partial z}$= 0.2, $\varphi = \pi/3$, $\varepsilon_1 = 0.1$, $\alpha = 0.1$ $\varepsilon_2 = 0.5$, M=1

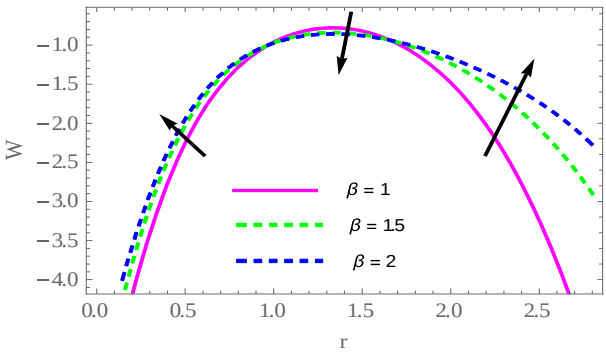

Fig. 3. Velocity distribution with different values of (β) z= 0.7, Gr= 2.0, $\phi = 0.04$, $\alpha = 0.1$, $\frac{\partial p}{\partial z}$= 0.2, $\varphi = \pi/3$, $\varepsilon_1 = 0.1$, $\varepsilon_2 = 0.5$, K= 0.5, M= 1

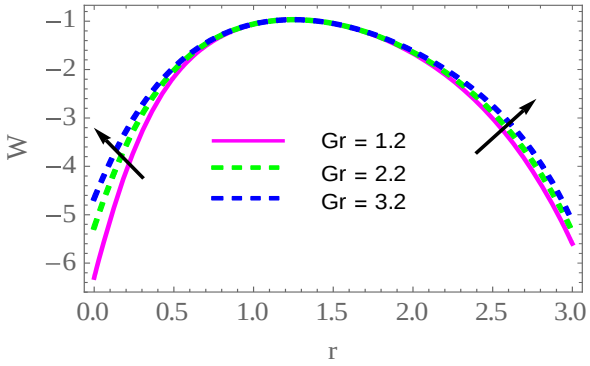

Fig. 4. Velocity distribution with different values of (Gr) z= 0.7, β= 2.0, $\phi = 0.04$, $\alpha = 0.1$, $\frac{\partial p}{\partial z}$= 0.2, $\varphi = \pi/3$, $\varepsilon_1 = 0.1$, $\varepsilon_2 = 0.5$, K= 0.5, M= 1

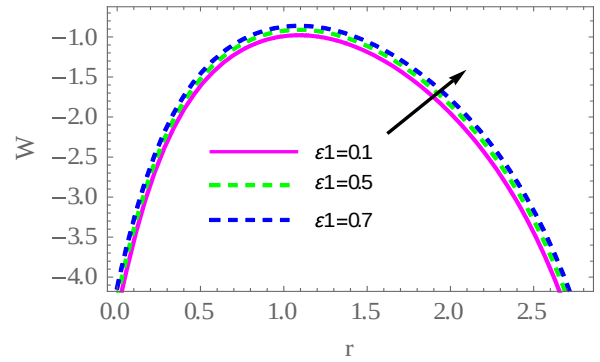

Fig. 5. Velocity distribution with different values of (ε_1) z= 0.7, Gr= 2.0, $\phi = 0.04$, $\beta = 2$, $\frac{\partial p}{\partial z}$= 0.2, $\varphi = \pi/3$, $\alpha = 0.1$, $\varepsilon_2 = 0.5$, K= 0.5, M= 1

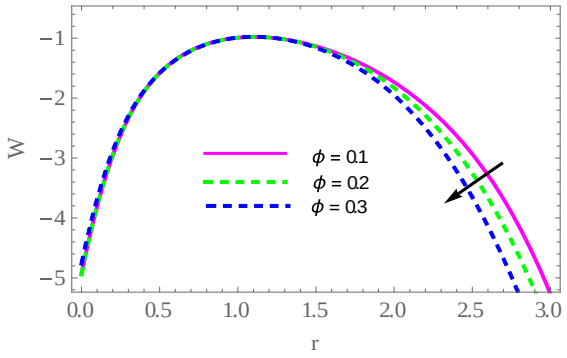

Fig. 6. Velocity distribution with different values of (ϕ) z= 0.7, Gr= 2.0, $\beta = 2$, $\frac{\partial p}{\partial z}$= 0.2, $\varphi = \pi/3$, $\alpha = 0.1$, $\varepsilon_1 = 0.1$, $\varepsilon_2 = 0.5$, K= 0.5, M= 1

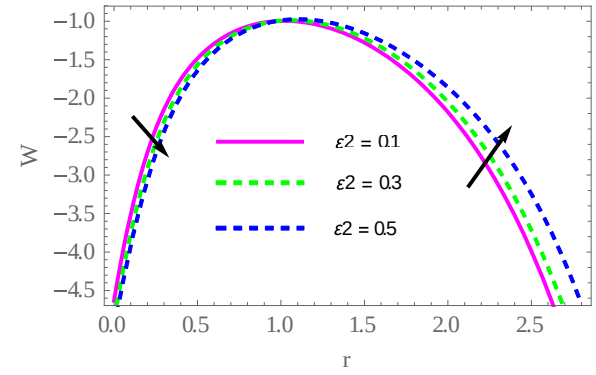

Fig. 7. Velocity distribution with different values of (ε_2) z= 0.7, Gr= 2.0, $\phi = 0.04$, $\beta = 2$, $\frac{\partial p}{\partial z}$= 0.2, $\varphi = \pi/3$,$\alpha = 0.1$, $\varepsilon_1 = 0.1$, K= 0.5, M= 1

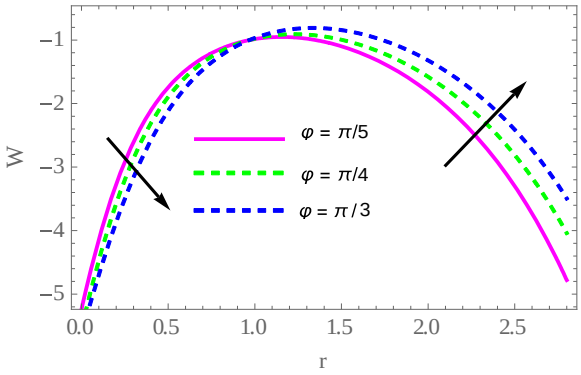

Fig. 8. Velocity distribution with different values of (φ) z= 0.7, Gr= 2.0, $\phi = 0.04$, $\beta = 2$, $\frac{\partial p}{\partial z}$= 0.2, $\varepsilon_1 = 0.1$, $\alpha = 0.1$, $\varepsilon_2 = 0.5$, K= 0.5, M= 1

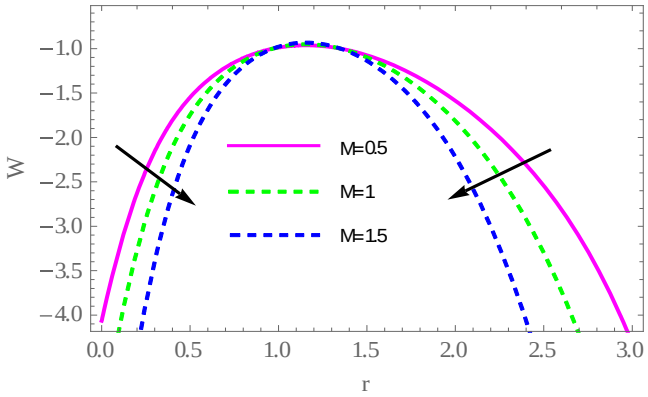

Fig. 9. Velocity distribution with different values of (M) z= 0.7, Gr= 2.0, φ=0.04, β=2, ∂p/∂z= 0.2, ϕ= π⁄3, α= 0.1, ε_1= 0.1, ε_2= 0.5, K= 0.5

4.2 Temperature Distribution

The Figure 10-14 clarify the effect of several physical parameters on fluid temperature distribution. Figure 10 shows result for the growing value of the heat source/sink parameter (β) tends to increasing in temperature profile. Figure 11 describes the variation in temperature for increasing values of the nanoparticle volume fraction (ϕ). It is remarkable to remind here that adding of nanoparticles and rising their volume fraction has considerable impacts on axial temperature of fluid. It is established that axial temperature decreases with increase in volume fraction of nanoparticles. In actuality, thermic conductivity of nanofluid is greater with the raise of nanoparticle volume fraction that smooth the heat transfer therefore decreasing the temperature. This is clear from decreasing temperature profile of the nanofluid with increases the nanoparticle volume fraction. From Figure 12, it was shown that the effect of amplitude of left wall (ε_1) on the temperature profile .The temperature increases with increase in (ε_1) .The behaviors of amplitudes of right wall (ε_2) and the phase difference (φ) on the temperature were illustrated in Figure 13 and 14, the temperature increases at right wall and in the middle.

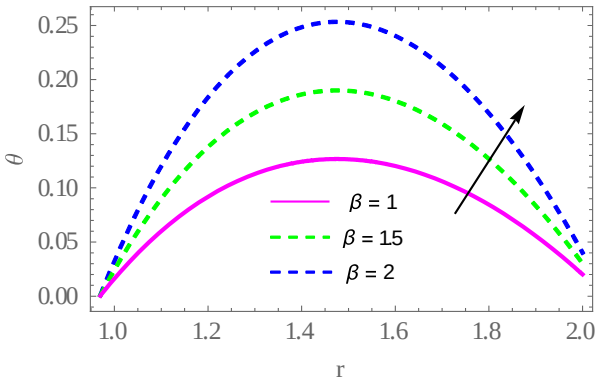

Fig. 10. Temperature profile with different values of (β) z= 0.7, $\phi = 0.04$, $\varphi = \pi/3$, $\varepsilon_1 = 0.1$, $\varepsilon_2 = 0.5$

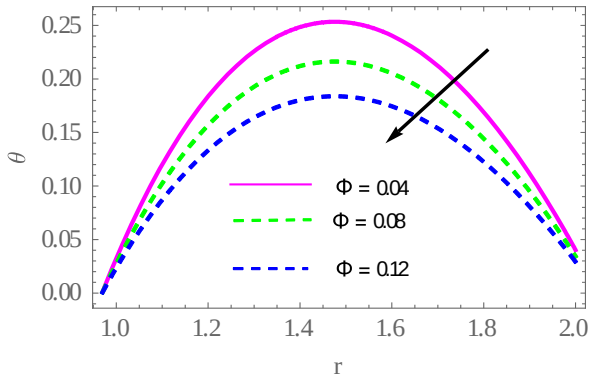

Fig. 11. Temperature profile with different values of (ϕ) z= 0.7, $\beta = 2.0$, $\varphi = \pi/3$, $\varepsilon_1 = 0.1$, $\varepsilon_2 = 0.5$

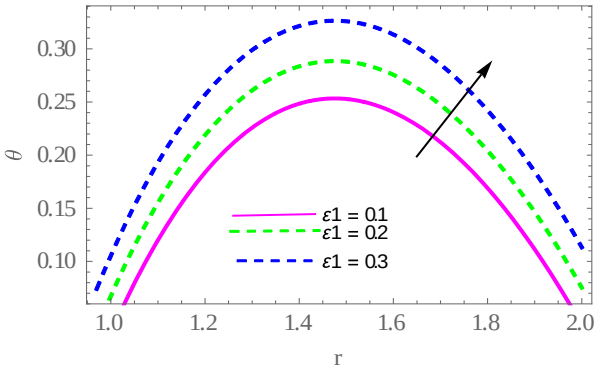

Fig. 12. Temperature profile with different values of (ε_1) z= 0.7,$\phi = 0.04$, $\varphi = \pi/3$, $\beta = 2.0$, $\varepsilon_2 = 0.5$

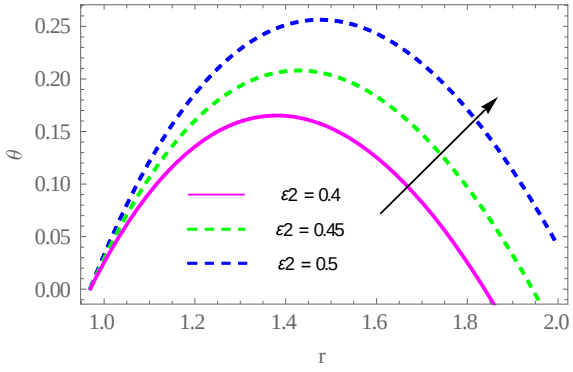

Fig. 13. Temperature profile with different values of (ε_2) z= 0.7, $\phi = 0.04$, $\varphi = \pi/3$, $\varepsilon_1 = 0.1$, $\beta = 2.0$

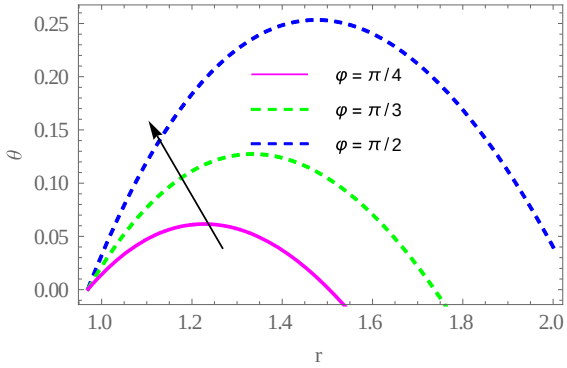

Fig. 14. Temperature profile with different values of (φ) z= 0.7, $\phi = 0.04$, $\beta = 2.0$, $\varepsilon_1 = 0.1$, $\varepsilon_2 = 0.5$

4.3 Heat Transfer Coefficient

Variance between temperature of fluid and temperature on the wall made the heat transfer coefficient occurs from wall to fluid. Heat transfer coefficient at the left wall of the tube Z_{h1} was taken graphically for several physical parameters through Figure 15-19. Z_{h1} is increasing the heat source/sink parameter(β) and the nanoparticle volume fraction (ϕ) effect is negligible (see Figure 15 and 16). Also one can note in Figure 17 the value of heat transfer coefficient decreases in region $(-0.25 < z < 0.25)$ and increases in the remaining region with the increasing of left wall amplitude $(\varepsilon 1)$. In Figure 18 we noticed that when $(z < 0)$ heat transfer coefficient increases with increasing the amplitude of right wall $(\varepsilon 2)$ but this behavior is reversed, when $z > 0$. Mixed behavior of the heat transfer coefficient is observed upon increasing the phase difference parameter (φ) via Figure 19.

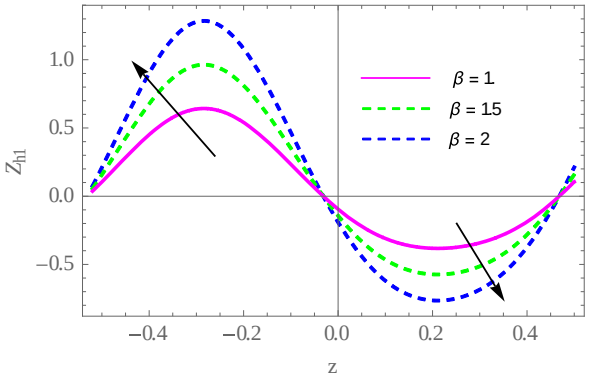

Fig. 15. Heat transfer coefficient with different values of $(\beta), \phi = 0.04, \varphi = \pi/3, \varepsilon_1 = 0.1, \varepsilon_2 = 0.5$

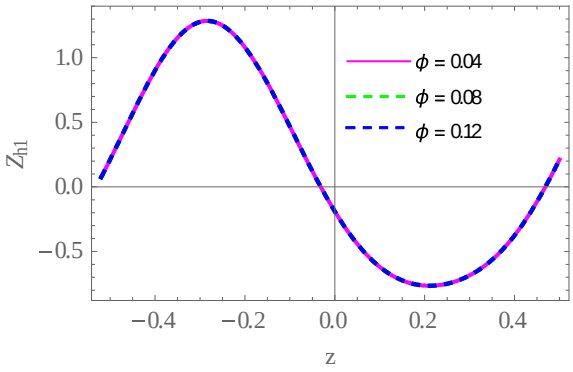

Fig. 16. Heat transfer coefficient with different values of $(\phi), \beta = 2.0, \varphi = \pi/3, \varepsilon_1 = 0.1, \varepsilon_2 = 0.5$

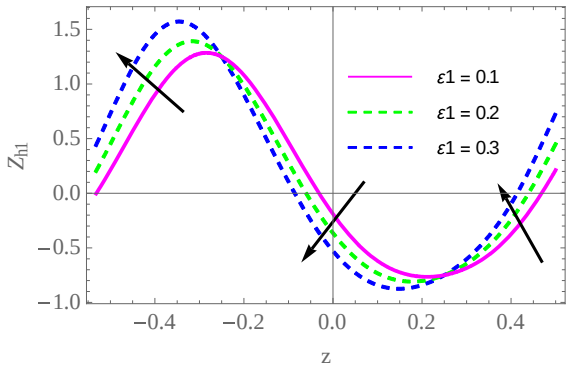

Fig. 17. Heat transfer coefficient with different values of $(\varepsilon_1), \phi = 0.04, \varphi = \pi/3, \beta = 2.0, \varepsilon_2 = 0.5$

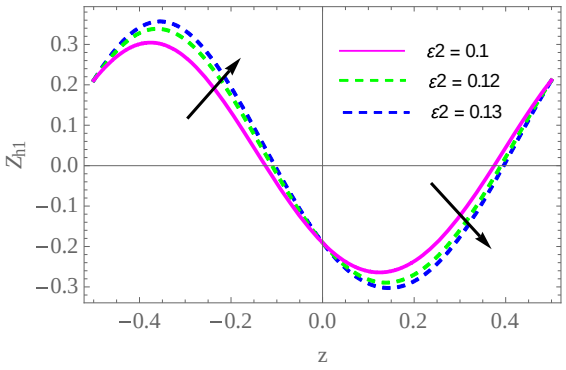

Fig. 18. Heat transfer coefficient with different values of $(\varepsilon_2), \phi = 0.04, \varphi = \pi/3, \varepsilon_1 = 0.1, \beta = 2.0$

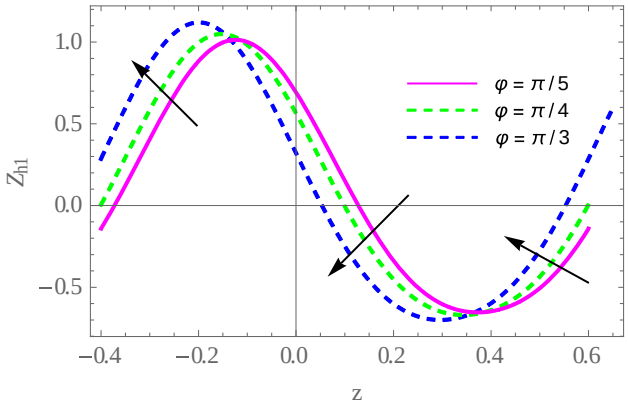

Fig. 19. Heat transfer coefficient with different values of $(\varphi), \phi = 0.04, \beta = 2.0, \varepsilon_1 = 0.1, \varepsilon_2 = 0.5$

5. Conclusions

In this mathematical model, we showed the effects of magnetic field and heat transfer on the peristaltic flow with a variable viscosity dependent on temperature through a porous medium in an asymmetric vertical tube. The governing equations are simplified under the suppositions of long- wavelength and low-Reynolds number. The approximate solution is obtained for velocity whereas the exact solution is obtained for temperature and heat transfer coefficient. We concluded the axial velocity increase at the walls with increasing of (α) and (Gr) parameters whereas nearly not affected in middle of center of tube. The axial velocity decreases at the center part of the channel with the increase in (β) and (K) while it enhances near the channel walls. It is observed that (M) has reverse influence and The CuO nanoparticles (ϕ) have virtually impact on the axial velocity close to the right wall and the velocity profile increase at the walls with increasing of (ε_1) . Increase in nanoparticles volume fraction (ϕ) shown decrease in temperature profile. The temperature distribution exhibits increase when ($\beta, \varepsilon_1, \varepsilon_2$),and ($\varphi$) increase. For different value of the parameters that control the heat transfer coefficient, it is related that the temperature increases up to limiting value of (z) and take opposite effect where (z) increase over that limiting value.

Acknowledgement
We gratefully acknowledge the support of the by the University of Baghdad, college of science, department of mathematics (mathematics laboratory).

References

[1] Shapiro, Ascher H., Michel Yves Jaffrin, and Steven Louis Weinberg. "Peristaltic pumping with long wavelengths at low Reynolds number." *Journal of fluid mechanics* 37, no. 4 (1969): 799-825.
[2] Latham, Thomas Walker. "Fluid motion in a peristaltic pump [MS thesis]." *Cambridge: Massachusetts Institute of Technology* (1966).
[3] Mekheimer, Kh S., and A. I. Abdellateef. "Peristaltic transport through eccentric cylinders: Mathematical model." *Applied Bionics and Biomechanics* 10, no. 1 (2013): 19-27.
[4] Nadeem, S., and Noreen Sher Akbar. "Exact and numerical simulation of peristaltic flow of a non-Newtonian fluid with inclined magnetic field in an endoscope." *International Journal for Numerical Methods in Fluids* 66, no. 7 (2011): 919-934.
[5] Reddy, G. Rami, and S. Venkataramana. "Peristaltic transport of a conducting fluid through a porous medium in an asymmetric vertical channel." *Journal of Advances in Applied Sciences* 2, no. 5 (2011): 240-248.
[6] Hayat, Tasawar, Nasir Ali, Saleem Asghar, and Abdul Majeed Siddiqui. "Exact peristaltic flow in tubes with an endoscope." *Applied Mathematics and Computation* 182, no. 1 (2006): 359-368.
[7] Akbar, Noreen Sher. "Entropy generation and energy conversion rate for the peristaltic flow in a tube with magnetic field." *Energy* 82 (2015): 23-30.
[8] Sheikholeslami, M., M. Gorji-Bandpy, D. D. Ganji, and Soheil Soleimani. "Heat flux boundary condition for nanofluid filled enclosure in presence of magnetic field." *Journal of Molecular Liquids* 193 (2014): 174-184.
[9] Vasudev, C., U. Rajeswara Rao, G. Prabhakara Rao, M. V. Subba. "Peristaltic flow of a Newtonian fluid through a porous medium in a vertical tube under the effect of a magnetic field." *Int J Cur Sci Res* 1, no. 3 (2011): 105-110.
[10] Rehman, Khalil Ur, M. Y. Malik, Mostafa Zahri, and M. Tahir. "Numerical analysis of MHD Casson Navier's slip nanofluid flow yield by rigid rotating disk." *Results in physics* 8 (2018): 744-751.
[11] Hayat, T., M. Rafiq, and A. Alsaedi. "Investigation of Hall current and slip conditions on peristaltic transport of Cu-water nanofluid in a rotating medium." *International Journal of Thermal Sciences* 112 (2017): 129-141.

[12] Masuda, Hidetoshi, Akira Ebata, and Kazumari Teramae. "Alteration of thermal conductivity and viscosity of liquid by dispersing ultra-fine particles. Dispersion of Al_2O_3, SiO_2 and TiO_2 ultra-fine particles." *Netsu Bussei* 7, no. 4 (1993): 227-233.
[13] Choi, Stephen US, and Jeffrey A. Eastman. *Enhancing thermal conductivity of fluids with nanoparticles*. No. ANL/MSD/CP-84938; CONF-951135-29. Argonne National Lab., IL (United States), 1995.
[14] Xuan, Yimin, and Qiang Li. "Investigation on convective heat transfer and flow features of nanofluids." *J. Heat transfer* 125, no. 1 (2003): 151-155.
[15] Das, Sarit Kumar, Nandy Putra, Peter Thiesen, and Wilfried Roetzel. "Temperature dependence of thermal conductivity enhancement for nanofluids." *Journal of heat transfer* 125, no. 4 (2003): 567-574.
[16] Heris, S. Zeinali, S. Gh Etemad, and M. Nasr Esfahany. "Experimental investigation of oxide nanofluids laminar flow convective heat transfer." *International Communications in Heat and Mass Transfer* 33, no. 4 (2006): 529-535.
[17] Iftikhar, Naheeda, Abdul Rehman, Hina Sadaf, and Muhammad Najam Khan. "Impact of wall properties on the peristaltic flow of Cu-water nano fluid in a non-uniform inclined tube." *International Journal of Heat and Mass Transfer* 125 (2018): 772-779.
[18] Mekheimer, Kh S., W. M. Hasona, R. E. Abo-Elkhair, and A. Z. Zaher. "Peristaltic blood flow with gold nanoparticles as a third grade nanofluid in catheter: Application of cancer therapy." *Physics Letters A* 382, no. 2-3 (2018): 85-93.
[19] Aly, Emad H., and Abdelhalim Ebaid. "Effect of the velocity second slip boundary condition on the peristaltic flow of nanofluids in an asymmetric channel: exact solution." In *Abstract and Applied Analysis*, vol. 2014. Hindawi, 2014.
[20] Hayat, Tasawar, Maimona Rafiq, Bashir Ahmad, and Saleem Asghar. "Entropy generation analysis for peristaltic flow of nanoparticles in a rotating frame." *International Journal of Heat and Mass Transfer* 108 (2017): 1775-1786.
[21] Hussain, Q., T. Latif, N. Alvi, and S. Asghar. "Nonlinear radiative peristaltic flow of hydromagnetic fluid through porous medium." *Results in Physics* 9 (2018): 121-134.
[22] Mekheimer, Kh S., and Y. Abd Elmaboud. "Peristaltic flow through a porous medium in an annulus: application of an endoscope." *Appl. Math. Info. Sci* 2, no. 1 (2008): 103-121.
[23] Salman, Mohammed R., and Ahmed M. Abdulhadi. "Influence of heat and mass transfer on inclined (MHD) peristaltic of pseudoplastic nanofluid through the porous medium with couple stress in an inclined asymmetric channel." In *Journal of Physics: Conference Series*, vol. 1032, no. 1, p. 012043. IOP Publishing, 2018.
[24] Abbasi, Fahad Munir, Tasawar Hayat, Bashir Ahmad, and Guo-Qian Chen. "Slip effects on mixed convective peristaltic transport of copper-water nanofluid in an inclined channel." *PLoS one* 9, no. 8 (2014): e105440.